The benefits of S-waves and multicomponent data for surface monitoring

Ben Dando, Pinnacle, a Halliburton Service, St Agnes, UK
ben.dando@pinntech.com
Kit Chambers, Pinnacle, a Halliburton Service, St Agnes, UK
Raquel Velasco, Pinnacle, a Halliburton Service, Houston, Tx, US
Stephen Wilson, Pinnacle, a Halliburton Service, Houston, Tx, US

Summary

In this study, we examine the effect of multicomponent data on surface imaging, by generating, then migrating synthetic seismograms, using a moment tensor source together with 3D P-wave and S-wave velocity models. We use a novel imaging method known as moment tensor migration imaging (MTMI) to produce images of the microseismic source. In addition to resolving ambiguities related to imaging the anisotropic radiation patterns, images for individual moment tensor components are produced and can be used to discriminate source properties.

Our experiments illuminate several features pertinent to surface monitoring. In the first case, the use of a P-wave only migration, from vertical component data, results in several spurious features in the moment tensor images, which are due to incomplete coverage of the focal hemisphere. Inclusion of 3C data whilst still using a P-wave only migration does not improve on the vertical component only result. However, including S-waves from the two horizontal components significantly reduces the amount of leakage between different moment tensor components and increases both vertical and lateral resolution of the imaging. This indicates that for MTMI, the use of 3C data, which includes both P and S-waves, provides the best solution for improving both imaging resolution and the determination of source parameters.

Data and Method

The experiment geometry is shown in *Figure 1*. The hypothetical array consists of 993 sensors distributed with a diameter of 4 km. The sensors are arranged with a spacing of 50 m inline and 250 m crossline. The synthetic source location, 2500 m beneath the array center, is also marked in the figure. 3C synthetic traces were generated for the given source-array geometry by propagating P and S wavefields through 3D P-wave and S-wave velocity models. To compute the synthetics we use a wavefront construction method (Chambers and Kendall, 2008), and include the effects of geometrical spreading and ray angles. The final input parameter is the source mechanism, for which we chose a double-couple source consistent with horizontal motion in the X direction on a vertical fracture plane (i.e. an entirely M_{xy} moment tensor).

The synthetics do not include attenuation effects. However, we would expect that the shorter wavelengths for the S-wavefield would result in a lower central frequency than was used for P (30 Hz).

Accordingly, we fix the central frequency for the S-wavefield to 15 Hz. This is broadly consistent with Birkelo (2012) who observed an S-wave dominant frequency of around 12 Hz in surface microseismic data.

Given the input synthetics, we constructed source images using moment tensor migration imaging (MTMI, (Chambers, 2012)). Unlike standard diffraction stack approaches applied in surface monitoring, (e.g. Duncan and Eisner, 2010), the MTMI algorithm constructs images for 6 individual moment tensor components as well as a sum of the squares of the values for each image (referred to as the source intensity). The procedure projects data onto moment tensor components prior to stacking, where the projection weights depend on ray traced parameters for rays leaving the receivers that are incident upon the image point. Consequently, the MTMI method has the advantage that it can be applied to single or multi-component data, for both P and S wavefields - either independently or combined. The technique can be used with a variety of different stacking functions (stacks, semblance, etc.), making it applicable for low SNR data. Furthermore, low SNR detectability is also improved by the concentration of the source intensity at one single image maximum rather than spread across several lobes due to the anisotropic nature of the source radiation pattern.

Results

Figure 2 shows the resulting MTMI images, where only vertical component data were used for migrating the P-wave. The source intensity image shows the source image is smeared vertically, as would be expected from the time to depth trade-off observed when using a surface network geometry.

The images for the individual MTMI components show the largest amplitude on the Mxy component, which is consistent with the input source. There are, however, significant anomalies present in all the other MTMI component images. We note that the background level of stack amplitude is anomalously high for the Mzz component. However, as this is uniformly high throughout the image volume, it is unlikely to influence the interpretation of source parameters. All of the moment tensor component images show lobes around the 'true' source position which is due to incomplete coverage of the focal hemisphere; we refer to this phenomenon as leakage.

Next, we examine the P-wave only migration obtained using the same sensor geometry, but with 3C sensors at each receiver position (see *Figure 3*). The result is very similar to that obtained using only the vertical component data. The only observable difference is the absolute stack amplitude values due to the higher channel count (higher fold).

Finally, in *Figure 4* we show the result of a combined P and S-wave migration. In this case, vertical component data were used for the P-wave, whilst the S-wave was used from the two horizontal components at each sensor. The source intensity image of the P+S migration shows a much improved resolution to the P-wave only images, with significantly reduced vertical smearing. Using the 50% amplitude contour for the source intensity images, the depth range of the smearing is reduced from 160 m in *figure 2* to 110 m in *figure 4* (31%). Laterally the range is reduced from 70 m to 20 m (71%). In addition, the leakage in the combined P and S image has been significantly reduced. The only spurious feature created in the moment tensor component images is on the Mxz component, which is minimal relative to the P-wave only images; all other artefacts appear to be removed.

Conclusions

Our results show that the inclusion of S-waves from multicomponent data significantly improves imaging resolution. Leakage caused by incomplete focal hemisphere coverage, which is inherent for microseismic monitoring, is also significantly reduced.

The benefits of P vs P+S imaging are influenced by data quality, array geometry, and frequency content, and further work is required to explore the complexities and opportunities these will introduce. However, we expect improvement in resolution to be most significant for narrower aperture arrays, where the addition of the S-wave information will provide valuable depth constraints. Although several factors of note have not been included in this study, including free surface effects, anisotropy and finite frequency propagation, a number of key conclusions can be made.

The similarity between results for the P-wave migrations using only vertical component and then 3C data, suggests that multicomponent data does not improve imaging resolution for P-wave only migrations. However, detectability is improved because of the higher channel count.

In contrast, the addition of S-wave data significantly improves our imaging results. An increase in resolution is shown by a reduction in vertical and lateral smearing of 31% and 71% respectively. Furthermore, the addition of S-wave information in the imaging procedure removes all the spurious features except for minimal leakage onto the Mxz component – a result of the denser sensor spacing in the y-direction – providing a better basis for source characterization.
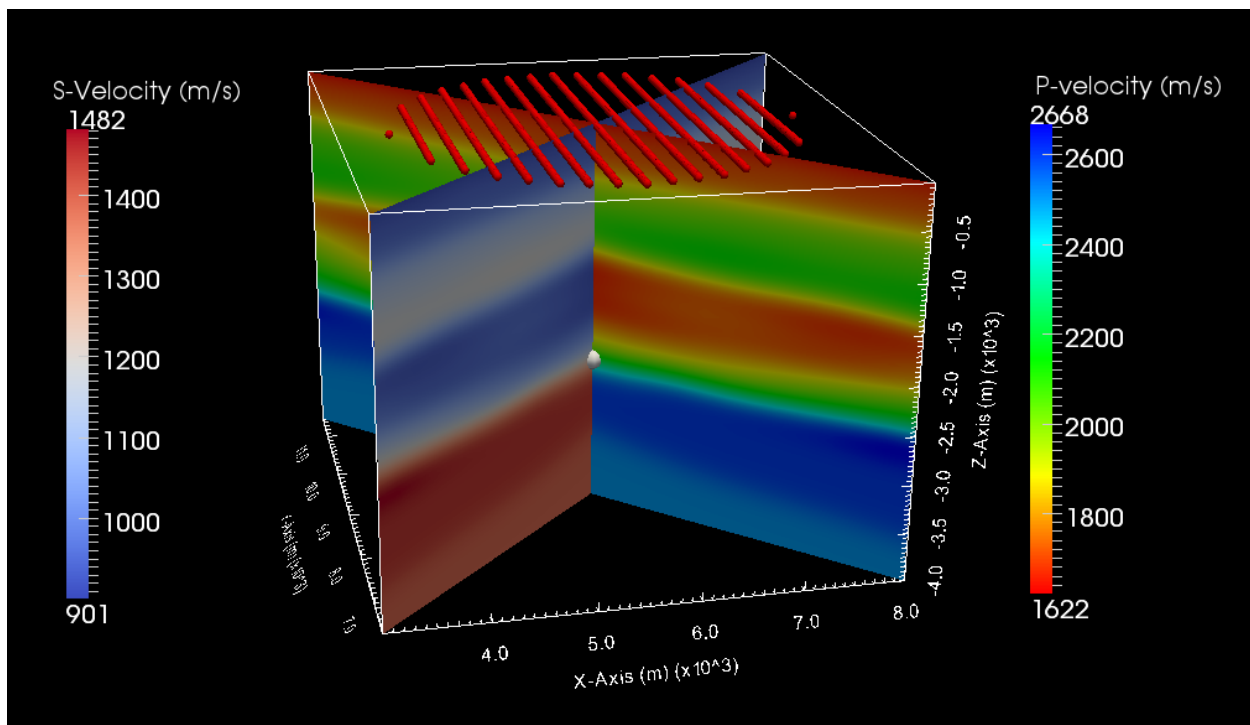
Acknowledgements

Figures

Figure 1: Overview of the experiment geometry. Red spheres show the sensor positions, producing an array with a diameter of 4000 m. Color panels show the 3D P-wave and S-wave velocity models used in this study. A white sphere marks the source location at 2500 m beneath the center of the array.
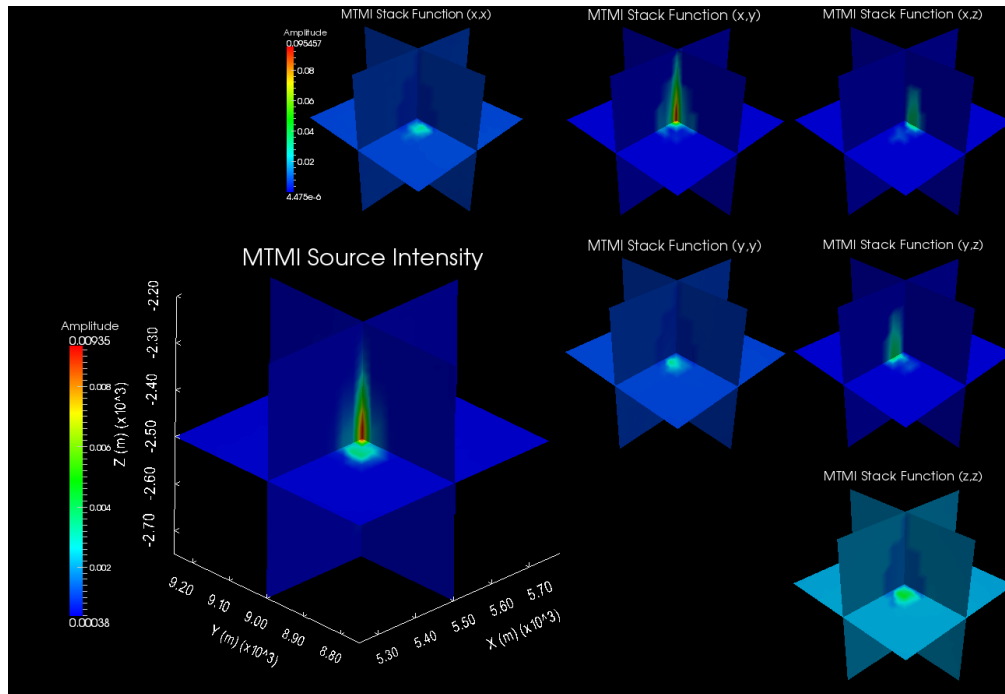

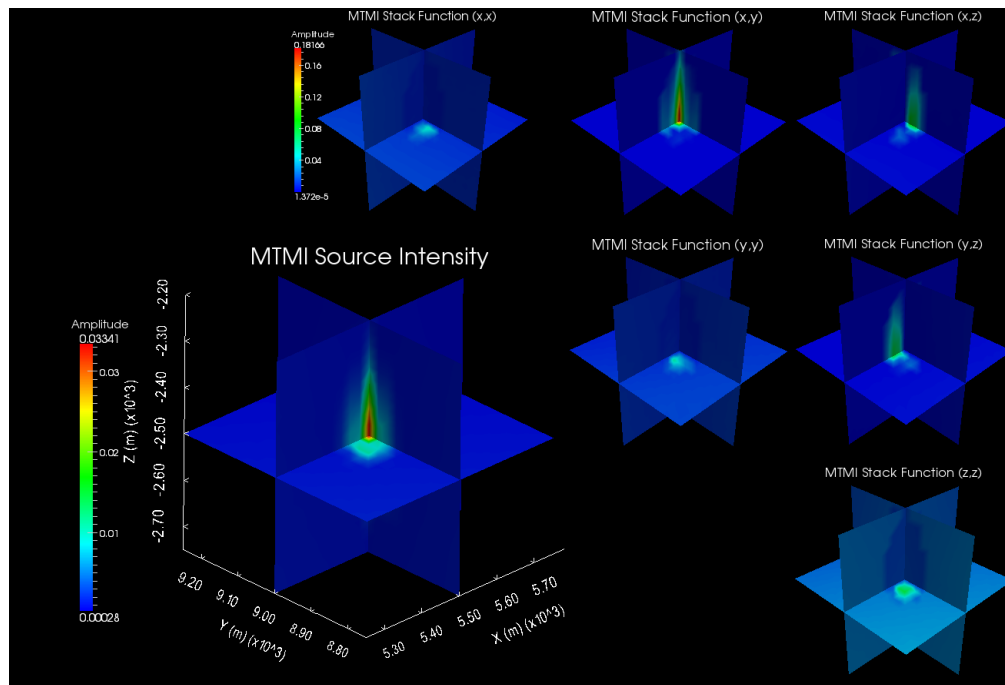Figure 2: MTMI stack function images generated by using a P-wave migration of the vertical component data.

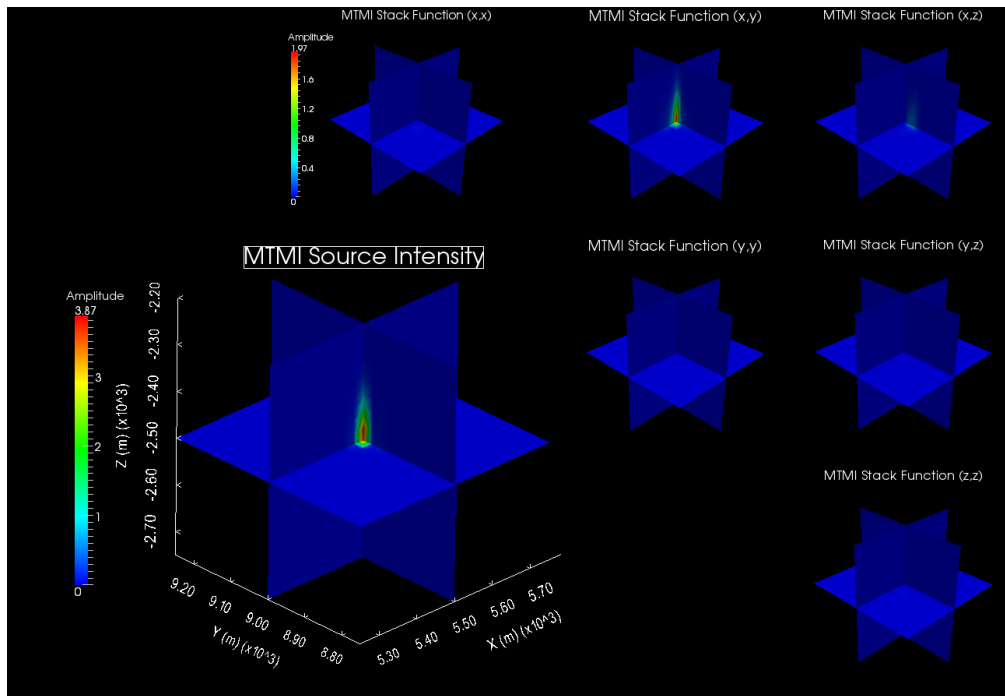Figure 3: MTMI stack function images generated by using a P-wave migration of the 3C data.

Figure 4: MTMI stack function images generated by using a combined P-wave and S-wave migration. The migration used the vertical component data for the P-wave, whilst data from the two horizontal components were used for the S-wave.

References

Birkelo, B., Cieslik, K., Witten, B., Montgomery, S., Artman, B., 2012. High Quality surface microseismic data illuminates fracture treatments: A case study in the Montney: The Leading Edge, **1318**.

Chambers, K. and Kendall, J.M., 2008. A practical implementation of wave front construction for 3-D isotropic media: Geophysical Journal International, **173**(3), 1030-1038.

Chambers, K., Wilson, S. , 2012. System and Method for Moment Tensor Migration Imaging, PCT/US12/46058, USA.

Duncan, P.M. and Eisner, L., 2010. Reservoir characterization using surface microseismic monitoring: Geophysics, **75**(5).